IEEE Access
Multidisciplinary | Rapid Review | Open Access Journal

Received February 3, 2020, accepted February 20, 2020, date of publication February 24, 2020, date of current version March 4, 2020.

Digital Object Identifier 10.1109/ACCESS.2020.2976195

Dynamic Control of a DFIG Wind Power Generation System to Mitigate Unbalanced Grid Voltage

ALI M. ELTAMALY[1,2,3], M. S. AL-SAUD[1,4], AND AHMED G. ABO-KHALIL[5,6]

[1]Saudi Electricity Company Chair in Power System Reliability and Security, King Saud University, Riyadh 11421, Saudi Arabia
[2]Sustainable Energy Technologies Center, King Saud University, Riyadh 11421, Saudi Arabia
[3]Electrical Engineering Department, Mansoura University, Mansoura 35516, Egypt
[4]Electrical Engineering Department, College of Engineering, King Saud University, Riyadh 11421, Saudi Arabia
[5]Department of Electrical Engineering, College of Engineering, Majmaah University, Almajmaah 11952, Saudi Arabia
[6]Department of Electrical Engineering, College of Engineering, Assuit University, Assuit 71515, Egypt

Corresponding author: Ahmed G. Abo-Khalil (a.abokhalil@mu.edu.sa)

This work was supported by the Deanship of Scientific Research at King Saud University, Riyadh, Saudi Arabia under Grant RG-1439-66.

ABSTRACT This paper presents an improved control strategy for a doubly-fed induction generator (DFIG) during unbalanced grid voltage conditions. The proposed strategy was applied in both synchronization and grid-connected conditions. The synchronization process is carried by controlling the extracted positive and negative sequence components of the stator q-axis voltage to follow the grid q-axis voltage. This strategy can be accomplished by controlling the positive and negative sequence components of the rotor d-axis current. By perturbing the rotor d-axis current, the stator EMF builds up and follows the grid voltage accurately. The stator frequency and the phase difference between the stator and grid voltage are compensated by adjusting the stator d-axis positive and negative voltage components to zero. After synchronization, the proposed control strategy focuses on regulating the average stator active and reactive power control by controlling the positive components of q and d-axis currents, respectively. The second target is to minimize the generator torque ripple by controlling the rotor negative sequence components. At the same time, the grid side converter is controlled to minimize the grid power pulsations to reduce the impact of the unbalanced grid voltage. This study focuses on enhancing the dynamics of DFIG during the unbalanced grid voltage by using Multivariable State Feedback (MSF) current controllers. Experiments are carried out to validate the performance improvement by using the proposed method. The simulation and experimental results showed superior performance of the proposed control strategy.

INDEX TERMS DFIG, synchronization, MSF, unbalanced voltage.

I. INTRODUCTION

As a result of a growing concern for the environment, efforts have been made to minimize the negative impact of generating electricity through the use of renewable energy, one of these efforts are aimed at generating energy from wind, which today is the one with the greatest penetration in the renewable energy market, with annual growth rates above 30 % [1]. This boom in wind power generation is linked to the progress that power electronics have had in the last three decades, which has led to the development of wind energy conversion systems (WECS) efficient, low cost and flexibility for interconnection with the power grid. WECS can be classified into two types: fixed speed and variable speed system.

With regard to variable speed, the DFIG is the most used where the size of the power converters is reduced since they are in the rotor circuit [2]. Unlike the full converter wind turbine system with the same capacity of generators and converters, DFIG's converters account for 30% of the generator capacity. In this study, the rotor winding is connected to the grid via a back-to-back converter. This converter is made up of a rotor side converter (RSC), a grid side converter (GSC) and a decoupling capacitor between both converters, as shown in Figure 1. The RSC controls the transfer of active and reactive power between the DFIG

The associate editor coordinating the review of this manuscript and approving it for publication was Sanjeevikumar Padmanaban.

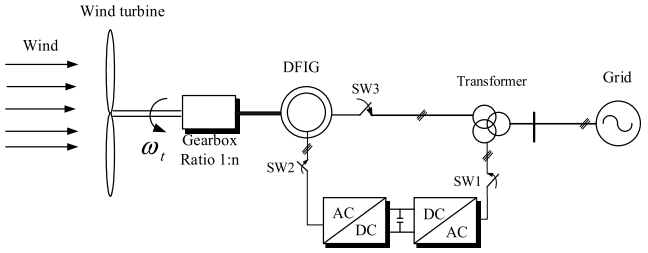

FIGURE 1. Grid-connected DFIG wind turbine.

stator and the network. While the GSC controls the reactive power between the converter and the network, in addition to taking care of the regulation of the DC link voltage [3]–[6]. In addition to the mentioned targets, there are other objectives of interest in the operation of DFIG, specifically those related to the quality of energy associated with certain grid disturbances [7].

In particular, in the case of the DFIG system, since the stator is directly connected to the grid, if an unbalance occurs in the grid, torque ripple occurs due to distortion of the rotor's rotor field. Torque ripple applies mechanical stress to wind power generation systems, causing mechanical failures in blades, gears and rotor shafts [8].

Even though, there are different control strategies for DFIG, field-oriented control (FOC) is the most popular controller which is used to control DFIG in normal operation conditions. The main advantages are the simplicity, reliability and the decoupling of the dynamics of the generator allowing to complement two independent regulators for active and reactive power [9]–[13]. However, conventional FOC techniques are not efficient in controlling DFIGs when grid disturbances occur. Several changes in the conventional FOC method have been introduced to reduce the effects of disturbances and improve the dynamic performance of the generator. First, to improve the conventional FOC technique, the positive and negative sequence components of the dq-axis rotor currents were regulated by using two additional proportional-integral PI current controllers. Tuning the four PI controllers, in addition to obtaining the positive and negative components from the dq-axis currents, complicates and slows the controllers' dynamic performance.

Many modifications have been introduced to improve the performance of FOC technique [14]–[20]. In [15] a PI current controller has been equipped with a resonant controller. PI controller and dual-frequency resonance have been combined together in [16]. These modification strategies are not accurate, and they are characterized by slow response due to their dependency on the DFIG parameters, the use of several reference frames, and the need for positive and negative sequence component extraction.

Advanced control strategies have been introduced to overcome these problems that directly control the unbalanced rotor currents without taking the positive or negative sequence components into consideration in the control system. These control systems use the extracted positive and negative sequence components instead of calculating sequence components of the current [17]. Predictive direct power control (PDPC) strategy has been used as another alternative to solve these problems [18]–[21]. In this strategy, during the switching period the stator active power, reactive power values, and lookup tables of two active vectors and one zero vector are applied. However, in a PDPC the negative sequence voltage and performance during voltage disturbances have not been taken into consideration. This idea will fasten the dynamic response especially in large power ripples and less control accuracy [22], [23].

On the other hand, controllers are developed by second-order sliding modes for a DFIG wind turbine, obtaining significant results such as the absence of chattering, convergence, and robustness with respect to external disturbances such as grid failures and with respect to non-modeled dynamics both in the turbine as well as in the generator [24]. Likewise, independently regulate the active and reactive generated power is developed by sliding modes [25]. Recently, passivity-based control (PBC) technique showed good results. A passive controller is developed based on the methodology called standard passivity-based control (S-PBC), which is based on a model developed from a representation on Euler-Lagrange and which aims to control a wind turbine with DFIG at its maximum power point to deliver the greatest amount of active power at each moment [26]. Another controller based on passivity is presented where, a Hamiltonian representation is used for the generator model, designing the controller based on the technique called Interconnection based passivity control and damping assignment (IDA-PBC) and considering the dynamics of the back-to-back converter [27].

In this paper, a Multivariable State Feedback (MSF) controller working with synchronous rotating coordinates is used to control the generator synchronization process to the grid by controlling the positive sequence of stator q-axis voltage using the main controller and the negative sequence component using an auxiliary controller. After connecting the generator to the grid, the RSC and GSC controllers are used to reduce the torques ripple and the active power ripples flowing into the grid. The 120-Hz components of the electromagnetic torque or stator reactive power is minimized by controlling the negative components of the rotor dq-axis currents. The experimental results show the capability of the proposed algorithm in reducing the impact of the unbalanced grid voltage on the DFIG torque and on the grid in both synchronization and running modes. Finally, the proposed current controller performance is compared to a PI controller in time of connection to the grid and during the normal operation.

II. DFIG CONTROL UNDER UNBALANCED VOLTAGE CONDITIONS

In balanced grid voltage condition, The RSC controls the transfer of active and reactive power between the DFIG stator and the grid. While the GSC controls the reactive power

between the converter and the grid, in addition to taking care of the regulation of the DC bus [3]–[6]. Generally, both converters (RSC and GSC), the current controllers are designed to guarantee the best dynamic performance, especially in WECS where the wind speed changes continuously and rapidly. However, in unbalanced grid voltage, it is necessary to mitigate the effect of the unbalanced voltage in the generator torque to reduce the stress on the mechanical parts and to make sure that the grid active power is free of ripple. In addition, it is important to guarantee smooth synchronization with equal grid and stator voltages. By using the grid and stator positive and negative sequence components, a smooth synchronization process can be obtained. After connecting the stator to the grid, the negative sequence components of the rotor should be set to zero to minimize the torque ripple. The GSC controller is used to control the DC link voltage and to minimize the grid active power ripple. The next sections show the details of the proposed method.

A. GENERATOR SIDE CONVERTER CONTRO

The vector diagram in Fig. 2 depicts the relationship between a stationary frame $\alpha_s\beta_s$ for the stator, rotor frame $\alpha_r\beta_r$ with rotating angular speed of ω_r, rotating frame for positive (dqp) at the angular speed of ω_s, and rotating frame for positive (dqn) at the angular speed of $(-\omega_s)$. The sequence components are represented by superscripts p and n represent, respectively. The value of the voltage, current, or flux can be expressed as a vector F in the stator-flux-oriented reference frame [34].

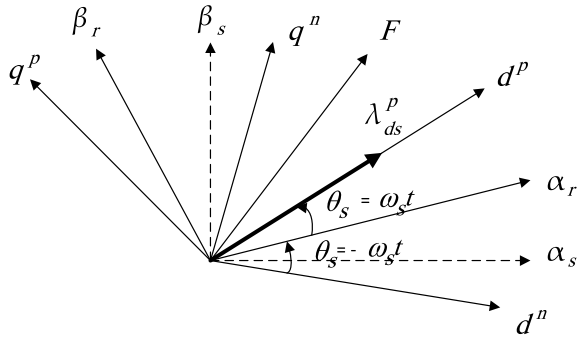

FIGURE 2. The positive and negative sequence components of dq-axis unbalanced vector.

If an unbalance occurs in the grid voltage, the apparent power of the stator can be expressed again in consideration of the unbalanced system:

$$S_s = \frac{3}{2}\left(v_{dqs}\cdot i^*_{dqs}\right) = \frac{3}{2}\left(e^{j\omega_e t}v^p_{dqs} + e^{-j\omega_e t}v^n_{dqs}\right)\cdot\left(e^{j\omega_e t}i^p_{dqs} + e^{-j\omega_e t}i^n_{dqs}\right) \quad (1)$$

In addition,

$$v^p_{dqs} = v^p_{ds} + j\,v^p_{qs}, \quad v^n_{dqs} = v^n_{ds} + j\,v^n_{qs},$$
$$i^p_{dqs} = i^p_{ds} + j\,i^p_{qs}, \quad i^n_{dqs} = i^n_{ds} + j\,i^n_{qs}.$$

Figure 3 shows the extraction process for the negative sequence components of the rotor dq-axis currents [24].

Eqs. (2) and (3) can be obtained by expressing the instantaneous active and reactive power of the stator by expanding Eq. (1) as shown in the following [35]–[38]:

$$P_s(t) = P_{s0} + P_{s\cos 2}\cos(2\omega_e t) + P_{s\sin 2}\sin(2\omega_e t) \quad (2)$$
$$Q_s(t) = Q_{s0} + Q_{s\cos 2}\cos(2\omega_e t) + Q_{s\sin 2}\sin(2\omega_e t) \quad (3)$$

The average and double frequency components of the active and reactive power can be written as follows:

$$\begin{bmatrix} P_{so} \\ P_{s\cos 2} \\ P_{s\sin 2} \\ Q_{so} \\ Q_{s\cos 2} \\ Q_{s\sin 2} \end{bmatrix} = 1.5 \begin{bmatrix} v^p_{ds} & v^p_{qs} & v^n_{ds} & v^n_{qs} \\ v^n_{ds} & v^n_{qs} & v^p_{ds} & v^p_{qs} \\ v^n_{ds} & -v^n_{qs} & v^p_{ds} & v^p_{qs} \\ v^p_{qs} & -v^p_{ds} & v^n_{qs} & -v^n_{ds} \\ v^n_{qs} & -v^n_{ds} & v^p_{qs} & -v^p_{ds} \\ -v^n_{ds} & -v^n_{qs} & v^p_{ds} & v^p_{qs} \end{bmatrix} \begin{bmatrix} i^p_{ds} \\ i^p_{qs} \\ i^n_{ds} \\ i^n_{qs} \end{bmatrix} \quad (4)$$

As shown in Eqs. (2) and (3), when an unbalance occurs in the grid voltage, the instantaneous active and reactive power of the stator are the direct components of P_{so} and Q_{so}. In addition, the magnitudes P_{scos2}, P_{ssin2}, Q_{scos2}, and Q_{ssin2} contain AC components that pulsate at a frequency that is double the power supply frequency. Because of this ripple component, the power of the stator pulsates, unlike in the equilibrium state. In a DFIG, the power of the stator is transferred directly to the system, so it is necessary to remove the pulsation. Eqs. (2) and (3) indicate that a power pulsation can be reduced by setting the magnitude of reactive power pulses to zero.

The dq-axis stator currents can be expressed as a function of the stator dq-axis flux and rotor dq-axis currents in sequence components:

$$i_{dqs} = \frac{1}{L_s}\left(\lambda_{dqs} - L_m i_{dqr}\right) \quad (5)$$

As described above, the DFIG control uses the stator flux reference coordinate system. Therefore, the d-axis voltage of each component of the positive and negative sequences is zero except for the voltage drop owing to the stator resistance. Therefore, assuming that the d-axis voltage of each component of the stator is zero, the magnitudes of the pulsating components of active and reactive power in Eq. (4) is expressed as a function of stator voltages. Replacing the stator dq-axis flux components, the active and reactive power components can be expressed as shown in (6).

$$\begin{bmatrix} P_{so} \\ P_{s\cos 2} \\ P_{s\sin 2} \\ Q_{so} \\ Q_{s\cos 2} \\ Q_{s\sin 2} \end{bmatrix} = \frac{1.5}{L_s} \begin{bmatrix} v^p_{ds} & v^p_{qs} & v^n_{ds} & v^n_{qs} \\ v^n_{ds} & v^n_{qs} & v^p_{ds} & v^p_{qs} \\ v^n_{ds} & -v^n_{qs} & v^p_{ds} & v^p_{qs} \\ v^p_{qs} & -v^p_{ds} & v^n_{qs} & -v^n_{ds} \\ v^n_{qs} & -v^n_{ds} & v^p_{qs} & -v^p_{ds} \\ -v^n_{ds} & -v^n_{qs} & v^p_{ds} & v^p_{qs} \end{bmatrix} \times \left(\frac{1}{\omega_e} \begin{bmatrix} v^q_{ds} \\ -v^p_{ds} \\ -v^n_{qs} \\ v^n_{ds} \end{bmatrix} - L_m \begin{bmatrix} i^p_{dr} \\ i^p_{qr} \\ i^n_{dr} \\ i^n_{qr} \end{bmatrix} \right) \quad (6)$$

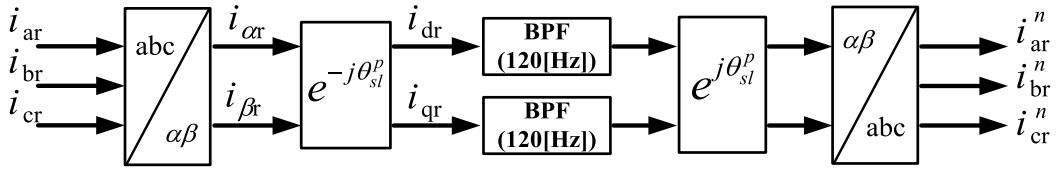

FIGURE 3. Extraction process of rotor negative sequence currents.

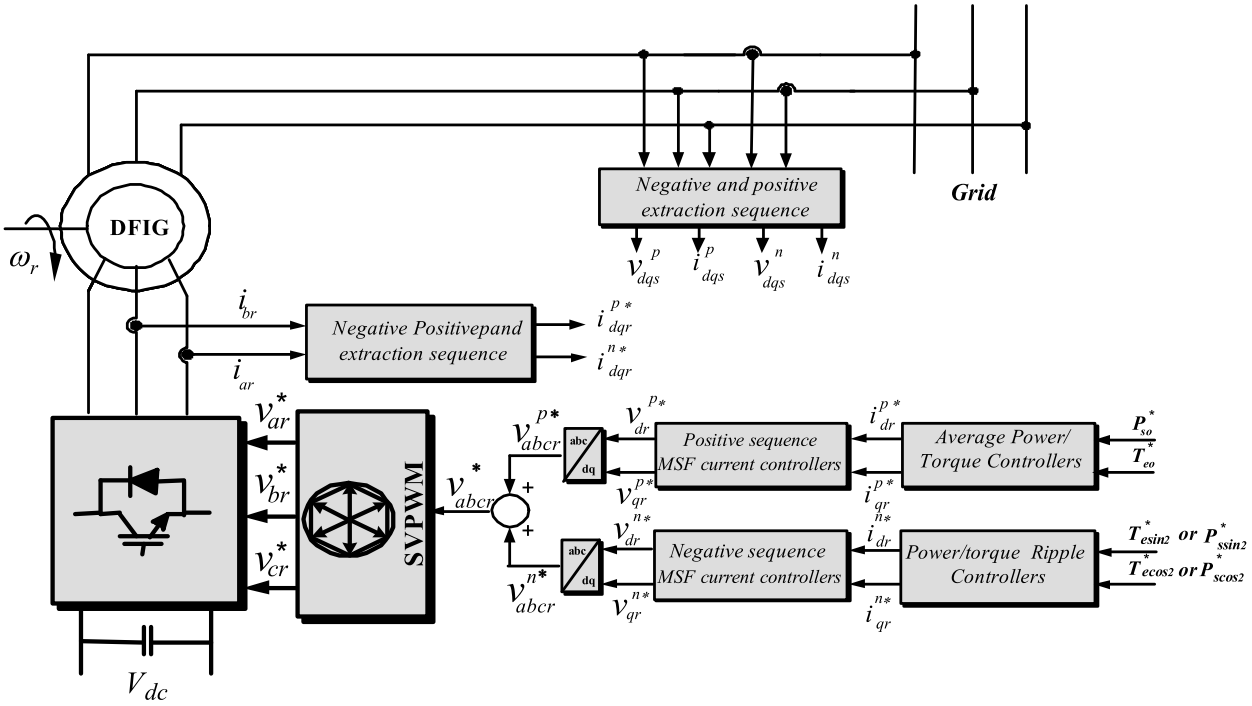

FIGURE 4. Power control diagram of rotor-side for unbalanced grid voltage.

where L_s is the stator inductance, L_m is the mutual inductance, ω_e is the electric frequency of the stator variables, ω_r the electric frequency of the rotor variables, v_{ds} is the voltage of the d-axis of the stator, v_{qs} is the voltage of the q axis of the stator.

The positive sequence components of the rotor currents, i^p_{dr} and i^p_{qr} are used to control the average torque and stator reactive power, while the negative components i^n_{dr} and i^n_{qr} are used to reduce the torque and power oscillations.

To minimize the oscillations in the stator active power, P_{scos2} and P_{ssin2} should equal zero. In this condition, the reference negative sequence components of the dq-axis rotor currents have to be adjusted from (6) as follows:

If the reactive power oscillation is required to be eliminated, then Q_{scos2} and Q_{ssin2} should equal zero. The reference rotor currents for this are as follows:

$$\begin{aligned} i^{n*}_{rd} &= \frac{1}{v^p_{sd}}\left(v^n_{sd}i^p_{rd} + v^n_{sq}i^p_{rq}\right) \\ i^{n*}_{rq} &= \frac{1}{v^p_{sd}}\left(v^n_{sd}i^p_{rq} - v^n_{sq}i^p_{rd}\right) \end{aligned} \tag{7}$$

The electromagnetic power of the DFIG in case of an unbalanced grid voltage can be expressed asshown in (8).

$$P_e(t) = -\frac{3}{2}\frac{L_m}{L_s}\left(P_{e0} + P_{ec2}\cos(2\omega_e t) + P_{es2}\sin(2\omega_e t)\right) \tag{8}$$

where, $P_{e0} = -v^p_{ds}i^p_{dr} - v^p_{qs}i^p_{qr} + v^n_{ds}i^n_{dr} + v^n_{qs}i^n_{qr}$

$$\begin{aligned} P_{e\cos 2} &= v^n_{qs}i^p_{dr} - v^n_{ds}i^p_{qr} + v^p_{qs}i^n_{dr} - v^p_{ds}i^n_{qr} \\ P_{e\sin 2} &= v^n_{ds}i^p_{dr} + v^n_{qs}i^p_{qr} - v^p_{ds}i^n_{dr} - v^p_{qs}i^n_{qr} \end{aligned}$$

The torque equation is expressed as shown in (9):

$$T_e(t) = p_n\frac{P_{e0}(t)}{\omega_e} \tag{9}$$

where p_n is the number of pole pairs.

$$\begin{bmatrix} T_{eo} \\ P_{e\cos 2} \\ P_{e\sin 2} \end{bmatrix} = -\frac{3p_nL_m}{2\omega_eL_s}\begin{bmatrix} -v^p_{ds} & -v^p_{qs} & v^n_{ds} & v^n_{qs} \\ v^n_{qs} & -v^n_{ds} & v^p_{qs} & -v^p_{ds} \\ v^n_{ds} & v^n_{qs} & -v^p_{ds} & -v^p_{qs} \end{bmatrix}\begin{bmatrix} i^p_{dr} \\ i^p_{qr} \\ i^n_{dr} \\ i^n_{qr} \end{bmatrix} \tag{10}$$

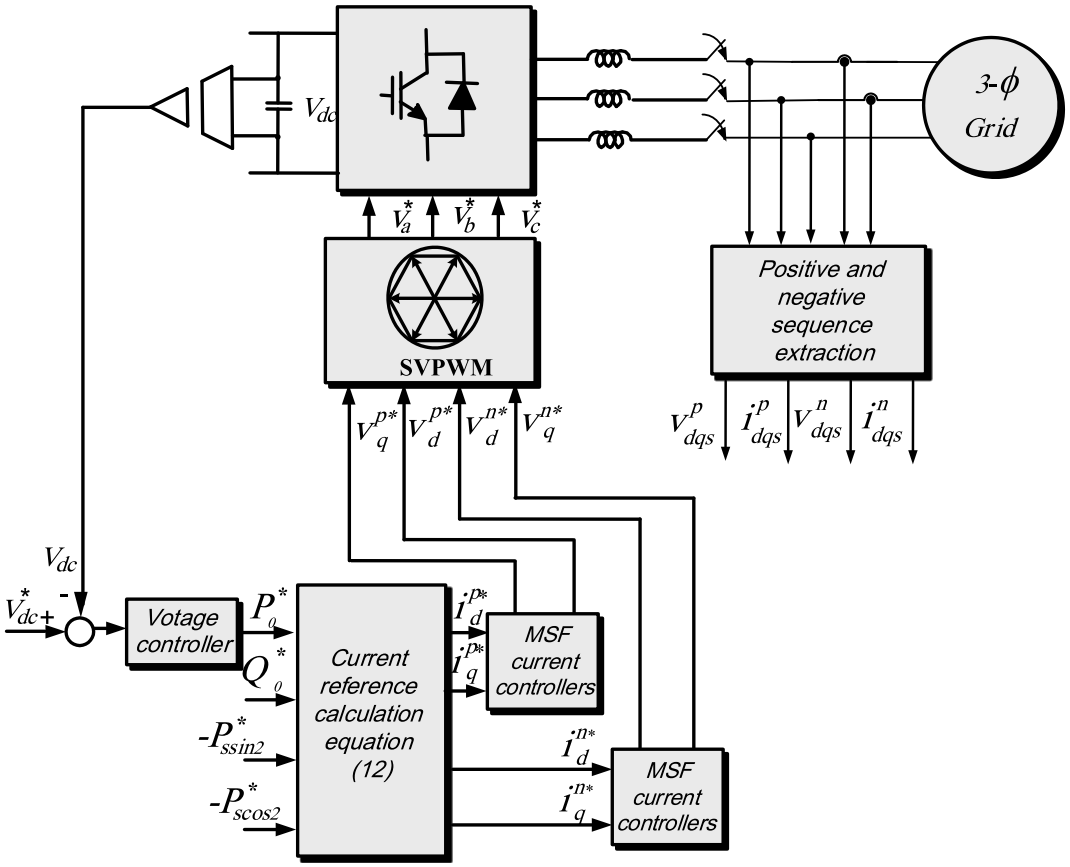

FIGURE 5. Control diagram of GSC under unbalance grid voltage.

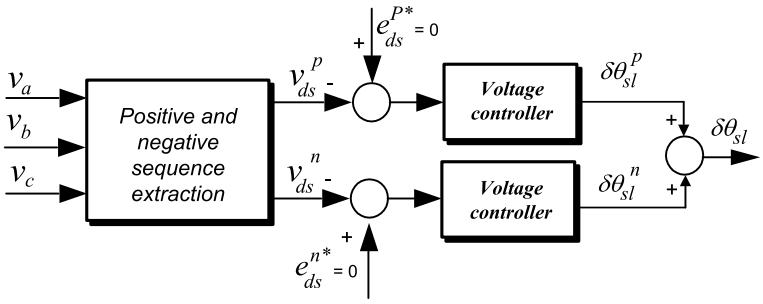

FIGURE 6. Phase difference compensation for synchronization.

To minimize the torque oscillation components T_{ecos2} and T_{esin2}, the reference negative sequence dq-axis rotor currents can be calculated from Eq. (10) as follows:

$$\begin{aligned} i_{rd}^{n*} &= \frac{1}{v_{sd}^p}\left(v_{sd}^n i_{rd}^p + v_{sq}^n i_{rq}^p\right) \\ i_{rq}^{n*} &= \frac{1}{v_{sd}^p}\left(v_{sd}^n i_{rq}^p - v_{sq}^n i_{rd}^p\right) \end{aligned} \tag{11}$$

It is clear that Eqns. (10) and (11) are identical which means that minimizing the torque ripples minimizes the reactive power ripples.

Figure 4 shows a power control diagram of the DFIG for an unbalanced grid voltage condition. The positive sequence components of the rotor currents i_{dr}^p and i_{qr}^p are used to control the average torque and stator reactive power, while the negative components i_{dr}^n and i_{qr}^n are used to reduce the torque and power oscillations.

B. GRID-SIDE CONTRO

In the stator side, the torque ripple control is applied to reduce the torque pulsations. However, the active power ripples flow into the grid without control that impacts the power quality of the grid currents. Such a situation is not desirable which

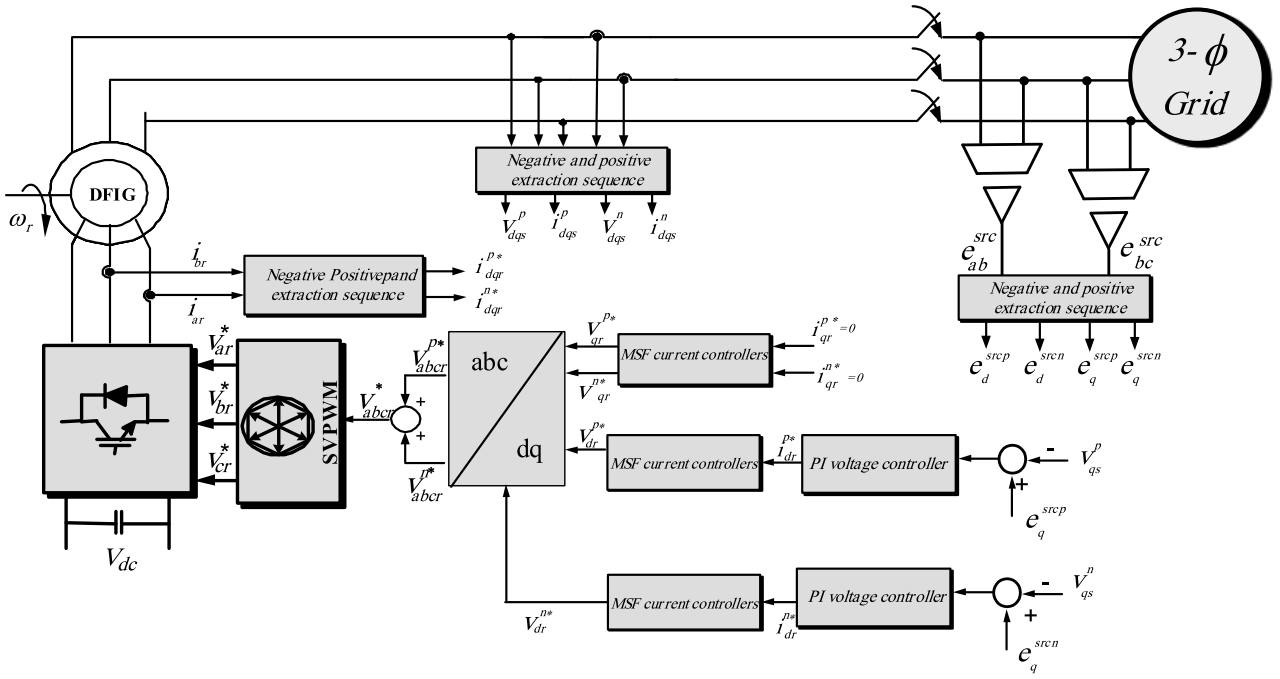

FIGURE 7. Synchronization of DFIG for unbalanced grid voltage.

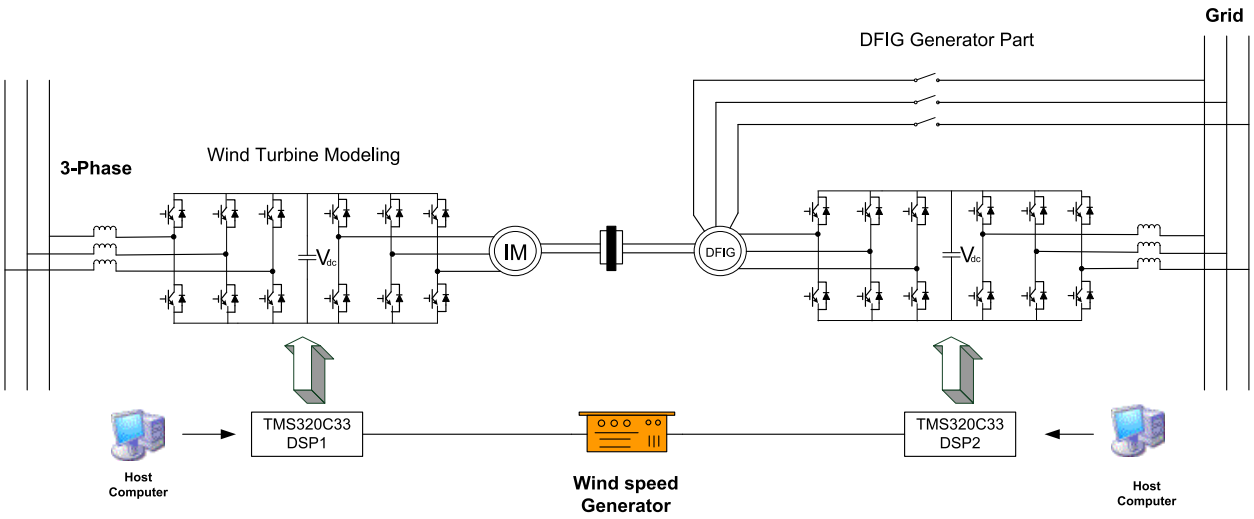

FIGURE 8. Schematic of experimental setup for DFIG connected to grid.

means the grid-side active power should be controlled to compensate the ripples.

The grid positive and negative sequence components of dq-axis currents references that are used to reduce the stator active power ripples can be derived as

$$\begin{bmatrix} i_d^{p*}(t) \\ i_q^{p*}(t) \\ i_d^{n*}(t) \\ i_q^{n*}(t) \end{bmatrix} = \begin{bmatrix} v_{ds}^p & v_{qs}^p & v_{ds}^n & v_{qs}^n \\ v_{qs}^p & -v_{ds}^p & v_{qs}^n & -v_{ds}^n \\ v_{qs}^n & -v_{ds}^n & -v_{qs}^p & v_{ds}^p \\ v_{ds}^n & v_{qs}^n & v_{ds}^p & v_{qs}^p \end{bmatrix}^{-1} \begin{bmatrix} 1.5P_0^* \\ 0 \\ -P_{ss2}^* \\ -P_{sc2}^* \end{bmatrix} \tag{12}$$

where P_0^* is the power reference for a constant DC voltage. Figure 5 shows the overall control diagram of the grid-side converter at an unbalanced grid voltage. The current controller consists of a positive sequence component controller and a negative sequence component controller, and the voltage controller to control the DC-link voltage.

C. SYNCHRONIZATION PROCESS CONTROL

The synchronization process in unbalanced grid voltage is similar to the process in balanced grid voltage except using additional negative sequence dq-axis current controllers to

compensate the unbalanced condition. In this case, the components of rotor d-axis currents are controlled to regulate the stator EMF to be as same as the grid voltage. The phase difference between the EMF and grid voltage is compensated by regulating the positive and negative sequence components of d-axis of the stator voltage to be zero, equally to the grid d-axis voltage, which produces the compensation component $\delta\theta_{sl}$ as shown in Fig. 6. The compensation component $\delta\theta_{sl}$ is then added to the slip angle to synchronize the stator voltage with the grid voltage. Then, the switch between the stator and grid is closed, and the generator is connected to the grid. The active power controller is then activated to regulate both the active and reactive power to the reference value. The overall control system for both synchronization mode and running mode in a balanced grid voltage is shown in Fig. 7. The positive and negative sequence components of the rotor currents are then controlled to regulate the stator active and reactive power and to minimize the torque ripples, respectively.

III. EXPERIMENTAL RESULTS

Figure 8 shows the schematic diagram of the experimental apparatus. It can be divided into DFIG for power generation and cage induction for turbine simulator. The specifications of the DFIG and the cage inductors are shown in Table 1 and 2 in the appendix.

The DFIG set can be further divided into an RSC and an GSC which are Semikron's 1200 [V] and 75 [A] IGBT power stacks. The gate driver is a Semikron SKHI 26W with internal insulation, and the communication with the control board is optical wire, which prevents the transfer of switching noise to the control board. Additionally, with the purpose of controlling the amount of active and reactive power injected into the power line, it is necessary to measure the current and voltage in two of the phases in the three-phase power line. The electrical signals used are:

- Two current signals in the RSC.
- Four current and four voltage signals in the GSC.
- DC link voltage signal.

LEM's LV25-P was used as the voltage sensor for measuring DC voltage, and L55's LA55-P was used for the grid, rotor and stator current sensors. Grid voltage and stator voltage were measured using a measuring transformer. Both control boards used TI's DSP TMS320VC33. The DSP has 32-bit floating point operations up to 120 (MFLOPS). It also features 14-bit A/D converters, digital inputs and outputs, and EPLDs that generate gating pulses. The switching frequency of the GSC and RSC of the DFIG is 5 kHz. Since the switching frequency is 5 kHz, the filter of the grid-side converter uses only a boost inductor (3 mH). DFIG's control board has many measurement signals, so the A/D converter has 12 channels and D/A is 4 channels.

For the experiments, the amplitudes of phase voltages e_{bs} and e_{cs} are reduced to produce an unbalanced grid voltage, as shown in Fig. 9 (a). The stator and rotor currents are shown in Fig. 9(b) and (c).

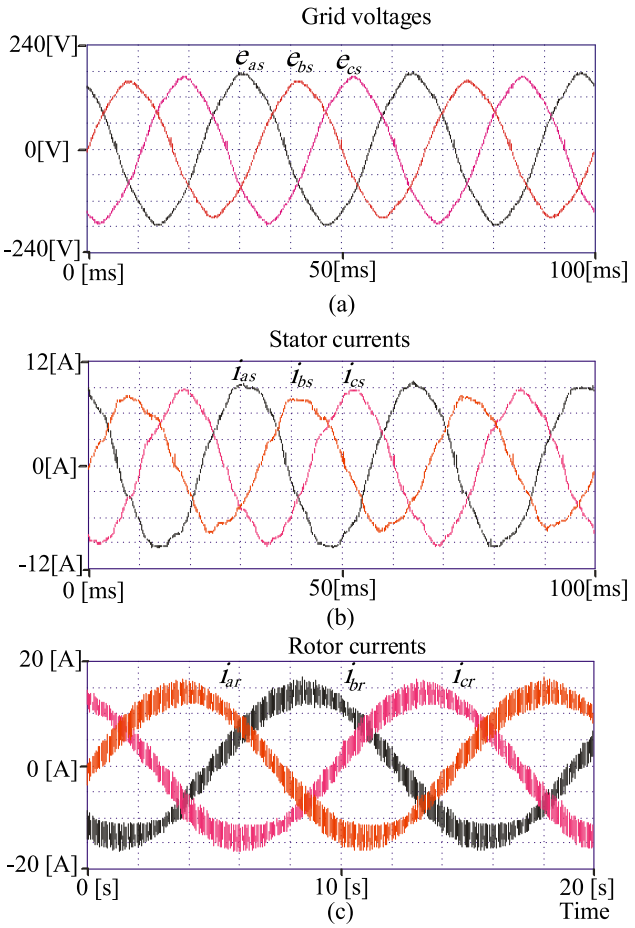

FIGURE 9. Unbalanced (a) grid voltages, (b) stator currents, (c) rotor currents.

Without regulating the stator active and reactive power, a double-frequency component fluctuates stator active and reactive power around the average. If the DFIG is controlled without any consideration of the unbalanced voltage, the active and reactive power oscillate around the reference values with a double frequency, as shown in Fig. 10 (a) and (b). The 120 Hz components of the stator active and reactive power are clearly in the harmonic spectrum of Fig. 11 (a) and (b). The grid active and reactive power will oscillate with the same frequency as shown in Fig. 12 (a) and (b). It can be seen that the unbalanced grid voltage causes the generator torque to have a 120 Hz frequency.

From Figure 13 (a) and (b), it is clear that, the conventional control scheme can't control the stator voltage to follow the grid voltage accurately. This drawback causes torque pulsations in the DFIG as well as power oscillations in the grid side.

Figure 14(a) and (b) clarifies the accuracy of the proposed method in synchronizing the stator voltage with the unbalanced grid voltage, thereby reducing the DFIG torque pulsations and grid power oscillations.

The first tested case is to eliminate the stator's active power. Figure 15 (a) shows the stator active power waveform after

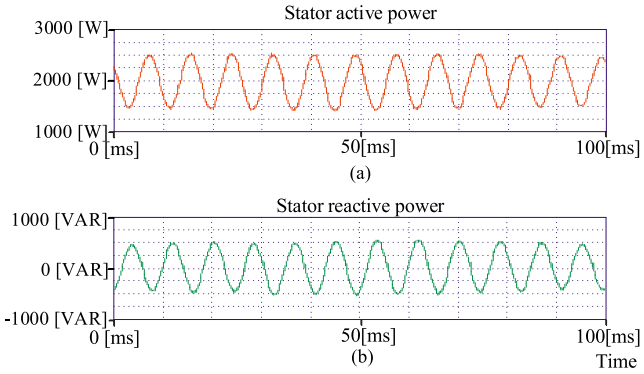

FIGURE 10. (a) Stator active power (b) stator reactive power under unbalanced voltages.

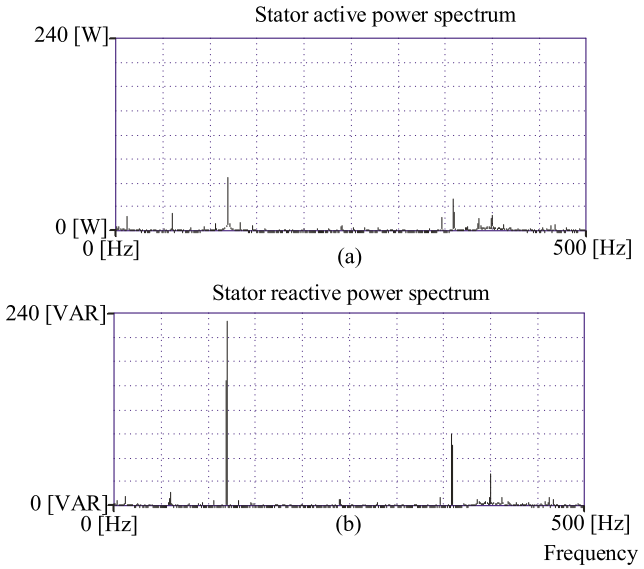

FIGURE 11. (a) Stator active and (b) reactive power harmonic spectrum for unbalanced grid.

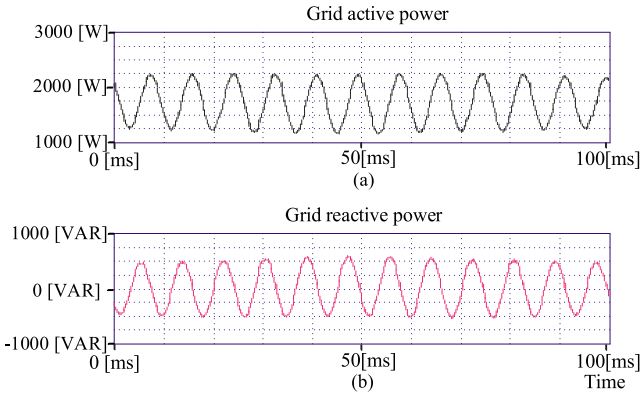

FIGURE 12. (a) Grid active and (b)reactive power under unbalanced voltages.

eliminating the double-frequency ripple component. The harmonic spectrum with no pulsation component at 120 Hz is shown in Fig. 16 (a). However, Fig. 15 (b) shows the

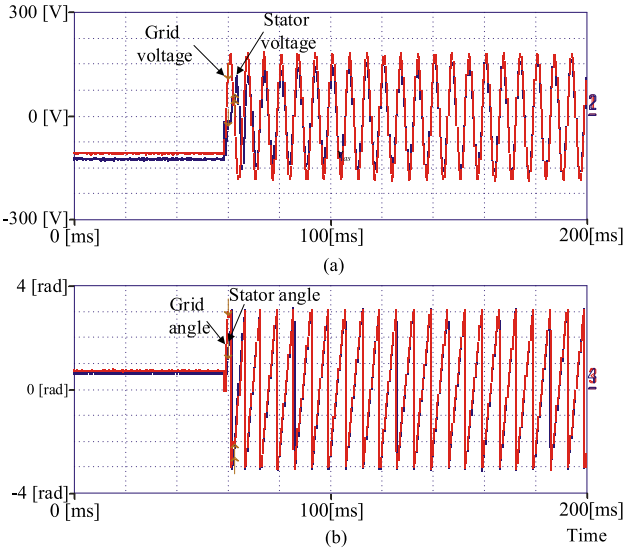

FIGURE 13. Grid and stator (a) voltages (b) phase angles with a conventional control scheme.

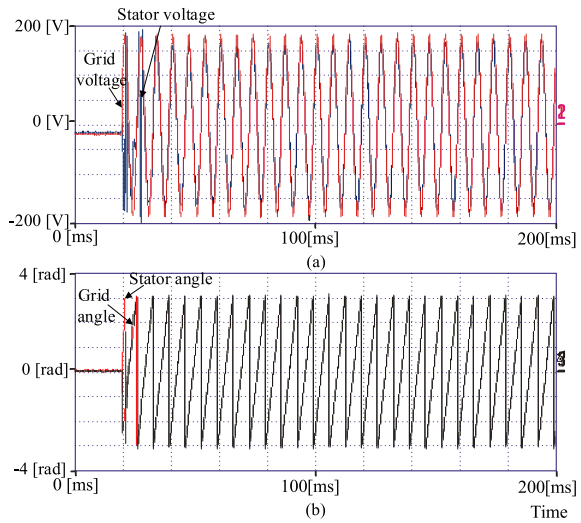

FIGURE 14. Grid and stator (a) voltages (b) phase angles with the proposed control scheme.

stator reactive power with noticeable ripples. Even though the average value is zero, the 120 Hz pulse component is high, as shown in Fig. 16 (b). Figure 15 (c) shows the torque waveform, which has peak-to-peak oscillations of about 1 Nm, while the generator speed oscillations are at about 1.1 rpm, as shown in Fig. 15 (d). Figure 16 (a) and (b) show the harmonic spectrum of the stator active and reactive power; respectively. The double frequency component is eliminated from the active power as shown in Fig. 16(a), while the same component exists in the stator reactive power in Fig. 16(b).

Figure 17 (a), (b), (c) and (d) show the rotor dq-axis currents of the positive and negative components when the stator active power ripples are controlled. It is noticeable that the performance of the proposed controller is efficient in regulating the rotor dq-axis currents with minimum oscillations.

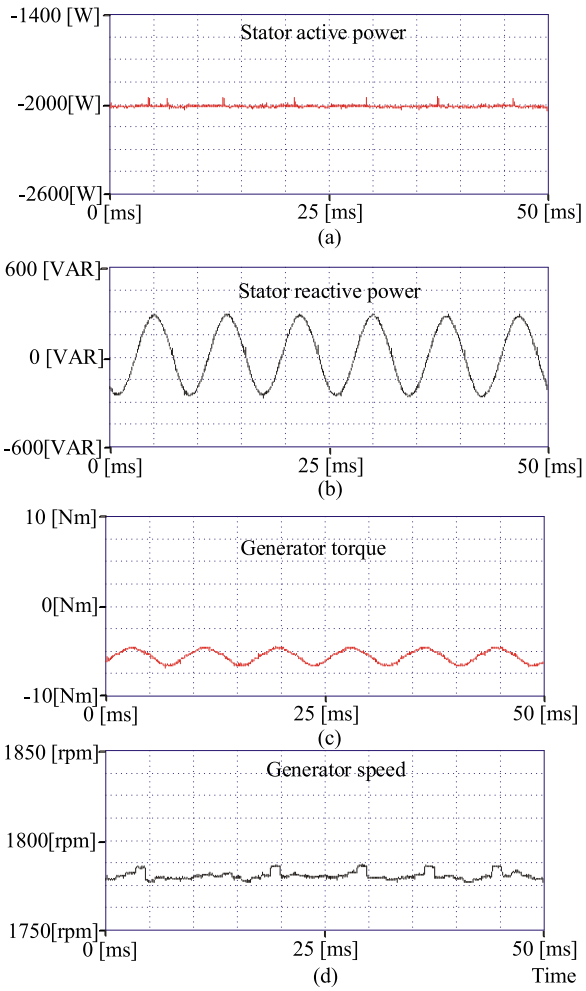

FIGURE 15. Generator speed for control eliminating ripple of stator active power: (a) stator active power, (b) stator reactive power, (c) generator torque, and (d) generator speed.

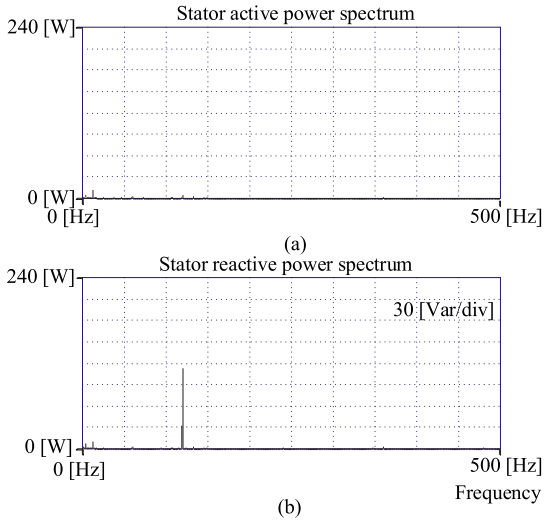

FIGURE 16. Harmonic spectrum of (a) stator active power and (b) stator reactive power.

In unbalanced grid voltage, the generator torque ripple can be reduced by controlling the stator reactive power ripple as shown in Fig. 18. This is the cause of the pulsation of the

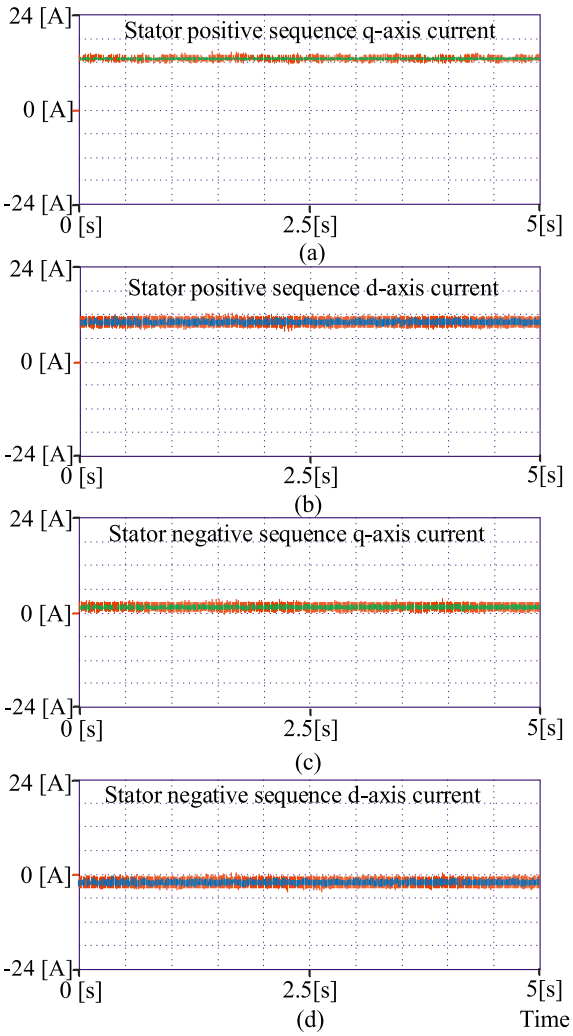

FIGURE 17. Rotor dq-axis reference and real currents of positive or negative components in active power ripple control using PI current controllers: (a) positive q-axis, (b) positive d-axis, (c) negative q-axis, and (d) negative d-axis.

total generated active power owing to the characteristics of the DFIG, and thus compensates through the GSC to prevent the active power ripple of the stator from being transmitted to the grid.

The stator active power, in Fig. 18(a), oscillates with the same magnitude since the ripple components of the stator active power are not compensated. However, the stator reactive power and torque ripple are reduced by controlling the sine and cosine components in (8) and (10). Figures 18 (b) and (c) shows the eliminated stator reactive power and generator torque ripple; respectively. The generator speed waveform in Fig. 18(d) shows reduced oscillations from the case of the conventional control method in Fig. 15(a). The grid active power ripple (12.6 W) in Fig. 19 (a) is reduced by compensating the stator active power ripple (234.6 W) in Fig. 12 (b) at the GSC. Figure 19 (c) and (d) show the reactive power of the GSC and RSC. Since the active power pulsation is compensated in the

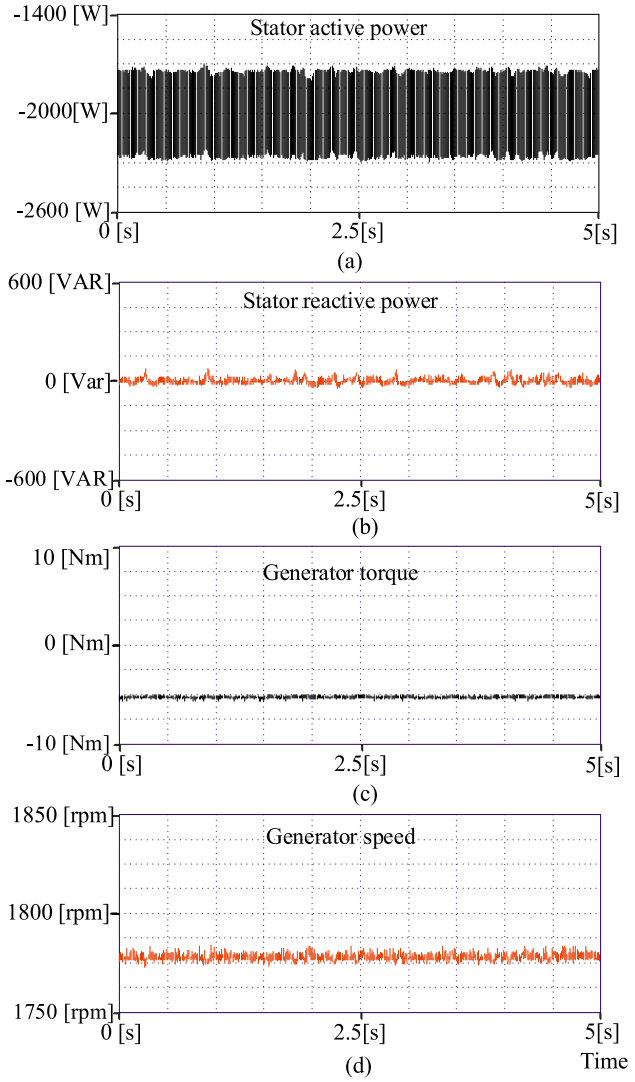

FIGURE 18. Generator torque for control to eliminate ripple using MSF current controllers: (a) stator active power, (b) stator reactive power, (c) generator torque, and (d) generator speed.

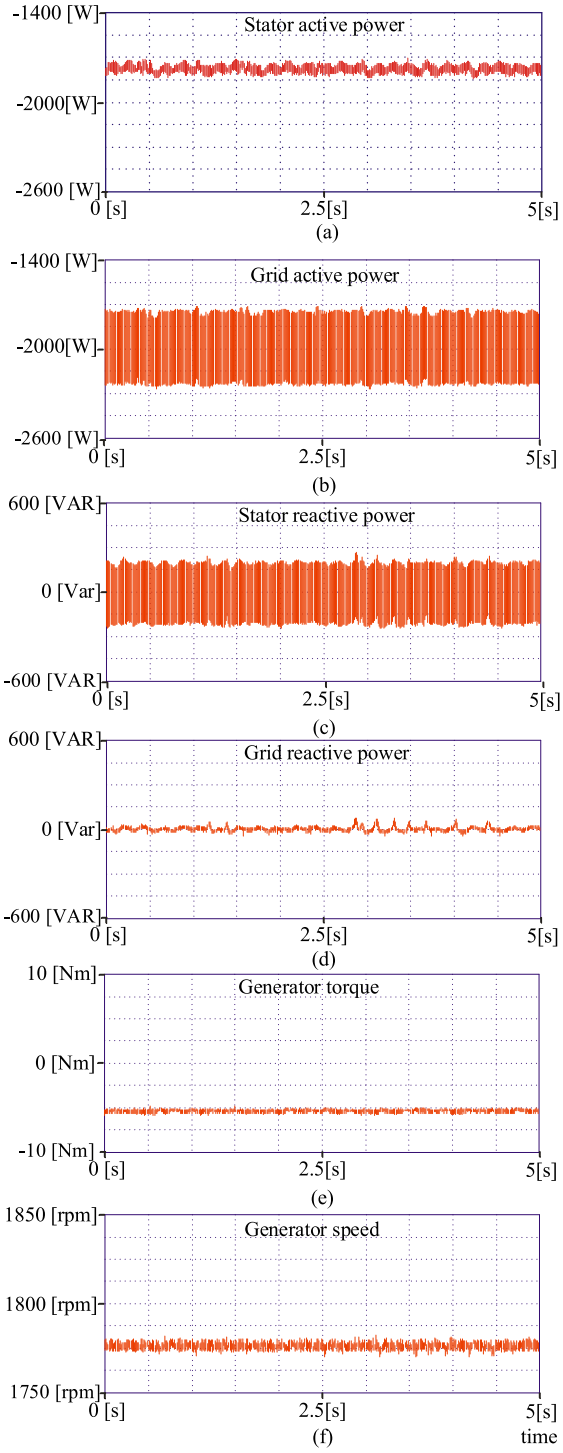

FIGURE 19. Grid active power to control elimination of ripple of grid active power: (a) grid active power, (b) stator active power, (c) grid reactive power, (d) stator reactive power, (e) generator torque, and (f) generator speed.

GSC, the pulsation (202.8 Var) of the reactive power is still in the GSC, which is transmitted to the grid. Figure 19 (e) shows the generator torque when the GSC is controlled to eliminate the active power pulsation of the grid side. The pulsation of the generator torque at this time is not much different from the one shown in Fig. 18 (c). Therefore, it can be seen that the reactive power pulsation of the grid occurs even if there is no reactive power pulsation of the stator, and it can be predicted that, the average value of the reactive power is zero, so it does not affect the power factor of the system. In addition, the generator speed in Fig. 19(f) shows higher oscillations more than the one shown in Fig. 18(d) because of the higher ripple of the generator torque.

A comparison between the proposed current controller and PI current controller is carried out to validate the robustness of the MSF controller in case of torque ripple control. Figure 20(a) shows the stator active power when a PI current controller is used. The power ripple is almost same as in MSF current controller in Fig. (18). However, the stator reactive power in Fig. 20(b) and the torque in Fig. 20(c) has a slightly higher ripple than the MSF controller in Fig. 18(b) and (c). The magnitude of the double-frequency components with PI

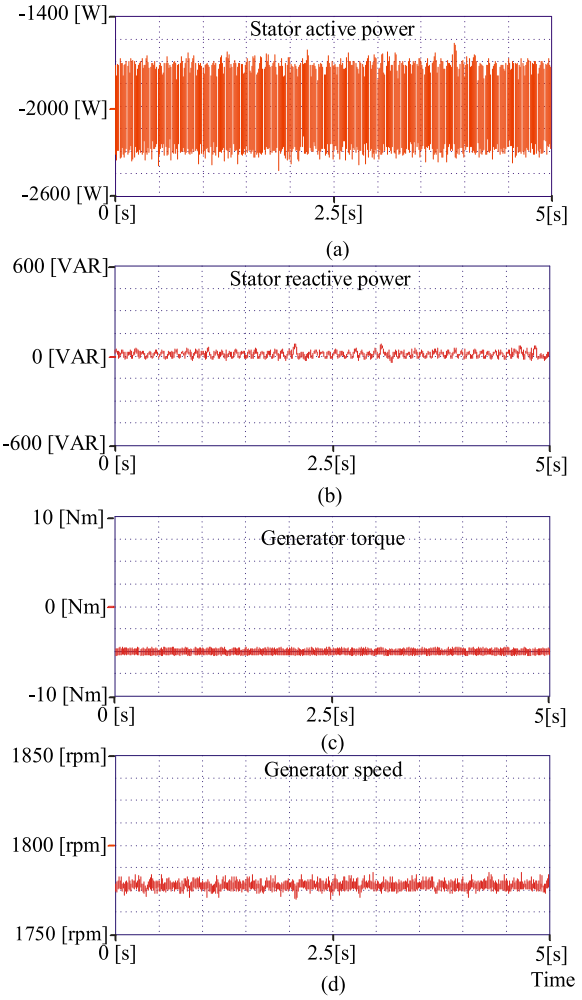

FIGURE 20. Generator torque for control to eliminate ripple using PI current controllers: (a) stator active power, (b) stator reactive power, (c) generator torque, and (d) generator speed.

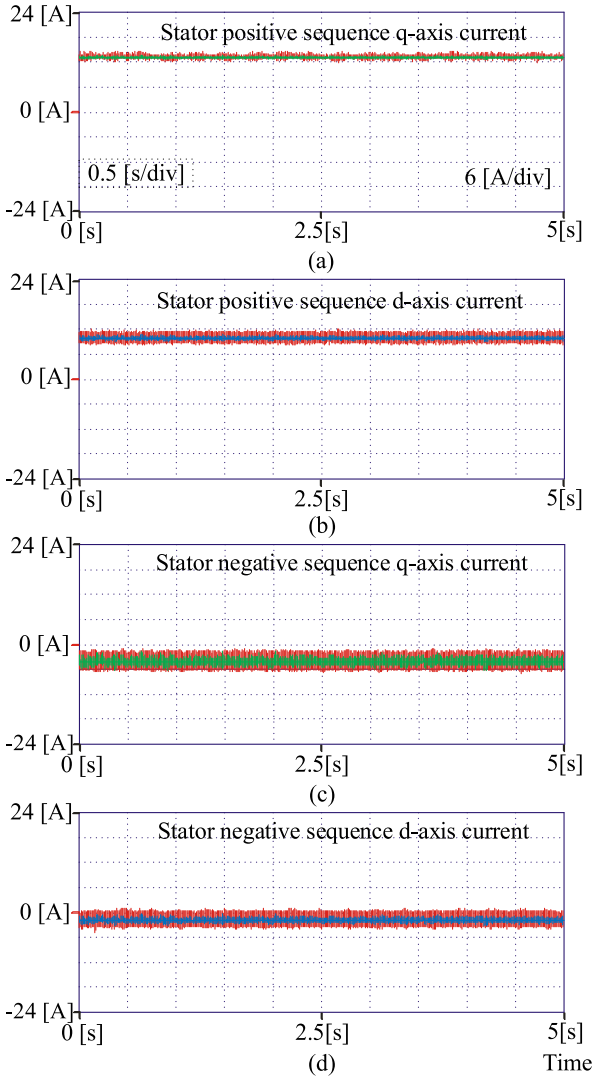

FIGURE 21. dq-axis rotor reference and real currents of positive or negative components in torque ripple control using PI current controllers: (a) positive q-axis, (b) positive d-axis, (c) negative q-axis, and (d) negative d-axis.

controller are 8 Var and 0.5 Nm, while in the MSF current controller are 5 Var and 0.35 Nm. The increase in the generator torque ripple reflects on the rotating speed in Fig. 20(d) which has an oscillation of 6 rpm compared with 4 rpm in case of MSF current controller in Fig. 18(d).

The control accuracy and robustness of the positive and negative dq-axis rotor currents is shown in Fig. 21. With a proper tuning for the gain of all current controllers, the positive components control in Fig. 21(a) and (b) is similar to the MSF in Fig. 17 (a) and (b). However, the negative sequence components show less robustness of PI controller as shown in Fig. 21(c) and (d). The magnitude of the peak to peak oscillation in the q-axis is 4 A which is higher than the case of MSF by 2 A, while d-axis current oscillation is 3 A which is higher than the MSF by 1 A.

It is noticeable that when the stator reactive power ripple is regulated to be minimum, the torque ripple reduced significantly. By controlling the sine and cosine components of the torque equation to be zero, the two negative sequence components of the rotor reference d and q-axis currents will minimize the torque ripple. From this, it was found that the magnitude of generator torque pulsation was related to the magnitude of stator reactive power pulsation. On the other hand, controlling the sine and cosine components of the stator active power to zero will reduce the active power pulsation without reducing the torque ripple. It can be seen obviously that, if the control tends to reduce the torque pulsation of the generator, the controller cannot reduce the active power pulsation of the stator. Due to the characteristics of the DFIG system, the active power pulsation of the stator is transmitted to the grid and the control method of the grid-side converter is proposed to compensate the active power pulsation in the grid side.

Finally, applying the proposed control technique to the DFIG wind power generation system can reduce the noise and mechanical stress compared to the conventional control method for the unbalanced power supply, and improve the

power generation reliability of the power generation system by controlling the grid-side converter.

IV. CONCLUSION

In this paper, MSF current controllers for RSC and GSC are designed and implemented for the generator torque pulsation and grid active power elimination of a DFIG under unbalanced operating conditions. Under an unbalanced grid voltage, the torque and power oscillations were fully defined, and the control targets to improve the system operation were discussed. The GSC outer DC link voltage controller is PI controller while the inner positive and negative dq-axis current controllers are MSF controllers. The proposed control algorithm separates the rotor current into positive and negative sequence components, to reduce the generator torque ripple, grid active power ripple and the DC-link voltage pulsation. The RSC is controlled to track the maximum power point with minimum torque ripple by using PI controllers while the inner current controllers are MSF controllers to regulate the rotor positive and negative dq-axis currents. While in the time of connecting DFIG to the grid, the RSC regulates the stator q-axis voltage components to reduce the impacts on the DFIG or grid in the synchronization time. The cascaded PI and MSF controllers guarantee strong and superior dynamics and fast transient responses.

By eliminating the generator torque pulsation, the stator reactive power pulsation was also eliminated. The grid power ripple is reduced to minimize the impacts of unbalanced voltage and currents on the grid. The analysis and experimental results showed that the proposed MSF current controllers of a DFIG can effectively suppress twice-multiplied frequency pulses of the electromagnetic torque, reactive power, and the active grid power under an unbalanced grid voltage.

The study presented a comparison between the conventional PI current controller and the MSF controller. After tuning the PI current controllers, the DFIG system runs in the same conditions in which the MSF current controllers are used. When the MSF current controller is compared to PI current controller, the first show better performance in the negative sequence components of rotor current control. In addition, the double frequency components in the stator reactive power and generator torque are higher in PI controller which indicates the superiority of the MSF current controller over the conventional PI controller. The slow dynamic performance of two consecutive PI controllers and the complications of tuning the controller gains deteriorate increase the currents and torque oscillations in an unbalanced grid voltage system which uses 4 current controllers in controlling the positive and negative components of rotor dq-axis currents.

APPENDIX

The specifications for the induction machine used for testing are as follows: three-phase, four poles, 230 [V], 50 [Hz], 3 [kW].

TABLE 1. Parameters of the turbine blade mode.

Parameters	Value
Blade radius	0.95 [m]
Max. power conv. coeff.	0.45
Optimal tip-speed ratio	7
Cut-in speed	4 [m/s]
Rated wind speed	13 [m/s]

TABLE 2. Parameters of the 3 kW Squirrel-Cage Induction Generator.

Parameters	Value
Stator resistance	0.93 [Ω]
Rotor resistance	0.533 [Ω]
Iron loss resistance	190 [Ω]
Stator leakage inductance	0.003 [H]
Rotor leakage inductance	0.003 [H]
Mutual inductance	0.076 [H]

REFERENCES

[1] P. B. Eriksen, T. Ackermann, H. Abildgaard, P. Smith, W. Winter, and J. M. R. Garcia, "System operation with high wind penetration," *IEEE Power Energy Mag.*, vol. 3, no. 6, pp. 65–74, Nov. 2005.
[2] M. Liserre, R. Cardenas, M. Molinas, and J. Rodriguez, "Overview of multi-MW wind turbines and wind parks," *IEEE Trans. Ind. Electron.*, vol. 58, no. 4, pp. 1081–1095, Apr. 2011.
[3] R. Cardenas, R. Pena, S. Alepuz, and G. Asher, "Overview of control systems for the operation of DFIGs in wind energy applications," *IEEE Trans. Ind. Electron.*, vol. 60, no. 7, pp. 2776–2798, Jul. 2013.
[4] G. Ramtharan, N. Jenkins, and J. B. Ekanayake, "Frequency support from doubly fed induction generator wind turbines," *IET Renew. Power Gener.*, vol. 1, no. 1, p. 3, 2007.
[5] A. G. Abo-Khalil and H. Abo-Zied, "Sensorless control for DFIG wind turbines based on support vector regression," in *Proc. 38th Annu. Conf. IEEE Ind. Electron. Soc. (IECON)*, Canada, Oct. 2012, pp. 3475–3480.
[6] Y. Song and H. Nian, "Sinusoidal output current implementation of DFIG using repetitive control under a generalized harmonic power grid with frequency deviation," *IEEE Trans. Power Electron.*, vol. 30, no. 12, pp. 6751–6762, Dec. 2015.
[7] F. Blaabjerg, R. Teodorescu, M. Liserre, and A. V. Timbus, "Overview of control and grid synchronization for distributed power generation systems," *IEEE Trans. Ind. Electron.*, vol. 53, no. 5, pp. 1398–1409, Oct. 2006.
[8] S. Xiao, G. Yang, H. Zhou, and H. Geng, "Analysis of the control limit for rotor-side converter of doubly fed induction generator-based wind energy conversion system under various voltage dips," *IET Renew. Power Gener.*, vol. 7, no. 1, pp. 71–81, Jan. 2013.
[9] A. Abo-khalil, D.-C. Lee, and S.-H. Lee, "Grid connection of doubly-fed induction generators in wind energy conversion system," in *Proc. 5th Int. Power Electron. Motion Control Conf.*, vol. 2, pp. 1–5, Aug. 2006.
[10] S. Muller, M. Deicke, and R. W. De Doncker, "Doubly fed induction generator systems for wind turbines," *IEEE Trans. Ind. Appl.*, vol. 8, no. 3, pp. 26–33, May/Jun. 2002.
[11] A. G. Abo-Khalil, S. Alyami, K. Sayed, and A. Alhejji, "Dynamic modeling of wind turbines based on estimated wind speed under turbulent conditions," *Energies*, vol. 12, no. 10, p. 1907, May 2019.
[12] A. G. Abo-Khalil, *Impacts of Wind Farms on Power System Stability*. Rijeka, Croatia: InTech, 2013.
[13] A. G. Abo-Khalil, "Synchronization of DFIG output voltage to utility grid in wind power system," *Renew. Energy*, vol. 44, pp. 193–198, Aug. 2012.
[14] J. Hu, Y. He, L. Xu, and B. W. Williams, "Improved control of DFIG systems during network unbalance using PI–R current regulators," *IEEE Trans. Ind. Electron.*, vol. 56, no. 2, pp. 439–451, Feb. 2009.
[15] Y. Zhou, P. Bauer, J. A. Ferreira, and J. Pierik, "Operation of grid-connected DFIG under unbalanced grid voltage condition," *IEEE Trans. Energy Convers.*, vol. 24, no. 1, pp. 240–246, Mar. 2009.
[16] D. Santos-Martin, J. L. Rodriguez-Amenedo, and S. Arnalte, "Direct power control applied to doubly fed induction generator under unbalanced grid voltage conditions," *IEEE Trans. Power Electron.*, vol. 23, no. 5, pp. 2328–2336, Sep. 2008.

[17] G. Abad, M. Á. Rodríguez, G. Iwanski, and J. Poza, "Direct power control of Doubly-Fed-Induction-Generator-Based wind turbines under unbalanced grid voltage," *IEEE Trans. Power Electron.*, vol. 25, no. 2, pp. 442–452, Feb. 2010.

[18] R. Datta and V. T. Ranganathan, "Direct power control of grid-connected wound rotor induction machine without rotor position sensors," *IEEE Trans. Power Electron.*, vol. 16, no. 3, pp. 390–399, May 2001.

[19] L. Xu and P. Cartwright, "Direct active and reactive power control of DFIG for wind energy generation," *IEEE Trans. Energy Convers.*, vol. 21, no. 3, pp. 750–758, Sep. 2006.

[20] D. Zhi and L. Xu, "Direct power control of DFIG with constant switching frequency and improved transient performance," *IEEE Trans. Energy Convers.*, vol. 22, no. 1, pp. 110–118, Mar. 2007.

[21] S. Jou, S. Lee, Y. Park, and K. Lee, "Direct power control of a DFIG in wind turbines to improve dynamic responses," *J. Power Electron.*, vol. 9, no. 5, pp. 781–790, 2009.

[22] A. G. Abo-Khalil, A. Alghamdi, I. Tlili, and A. M. Eltamaly, "Current controller design for DFIG-based wind turbines using state feedback control," *IET Renew. Power Gener.*, vol. 13, no. 11, pp. 1938–1948, Aug. 2019.

[23] A. G. Abo-Khalil, *Control system of DFIG for Wind Power Generation Systems*. New York, NY, USA: Academic, 2015.

[24] B. Beltran, M. E. H. Benbouzid, and T. Ahmed-Ali, "Second-order sliding mode control of a doubly fed induction generator driven wind turbine," *IEEE Trans. Energy Convers.*, vol. 27, no. 2, pp. 261–269, Jun. 2012.

[25] M. Adjoudj, M. Abid, A. Aissaoui, Y. Ramdani, and H. Bounoua, "Sliding mode control of a doubly fed induction generator for wind turbines," *Rev. Roum. Sci. Techn. Electrotechn. Energ.*, vol. 56, pp. 15–24, 2011.

[26] A. Monroy, L. Alvarez-Icaza, and G. Espinosa-Pérez, "Passivity-based control for variable speed constant frequency operation of a DFIG wind turbine," *Int. J. Control*, vol. 81, no. 9, pp. 1399–1407, Sep. 2008.

[27] H. H. Song and Y. B. Qu, "Energy-based modelling and control of wind energy conversion system with DFIG," *Int. J. Control*, vol. 84, no. 2, pp. 281–292, Feb. 2011.

[28] Z. Chen, J. M. Guerrero, and F. Blaabjerg, "A review of the state of the art of power electronics for wind turbines," *IEEE Trans. Power Electron.*, vol. 24, no. 8, pp. 1859–1875, Aug. 2009.

[29] Y. Zhang, J. Hu, and J. Zhu, "Three-vectors-based predictive direct power control of the doubly fed induction generator for wind energy applications," *IEEE Trans. Power Electron.*, vol. 29, no. 7, pp. 3485–3500, Jul. 2014.

[30] F. Bianchi, H. De Batista, and R. Mantz, *Wind Turbine Control Systems: Principles, Modelling and Gain Scheduling Design*. New York, NY, USA: Springer-Verlag, 2007.

[31] A. G. Abokhalil, "Grid connection control of DFIG for Variable Speed Wind Turbines under Turbulent Conditions," *Int. J. Renew. Energy Res. (IJRER)*, vol. 9, no. 3, pp. 1260–1271, 2019.

[32] A. G. Abo-Khalil, S. H. Lee, and D. C. Lee, "Grid connection of doubly-fed induction generators in wind Energy conversion system," in *Proc. Power Electron. Motion Control Conf.*, vol. 2, pp. 1–5, Aug. 2006.

[33] A. G. Abo-Khalil, A. S. Alghamdi, A. M. Eltamaly, M. S. Al-Saud, P. R. P., K. Sayed, G. R. Bindu, and I. Tlili, "Design of state feedback current controller for fast synchronization of DFIG in wind power generation systems," *Energies*, vol. 12, no. 12, p. 2427, Jun. 2019.

[34] H.-G. Park, A. G. Abo-Khalil, D.-C. Lee, and K.-M. Son, "Torque ripple elimination for doubly-fed induction motors under unbalanced source voltage," in *Proc. 7th Int. Conf. Power Electron. Drive Syst.*, Nov. 2007, pp. 1301–1306.

[35] T. Brekken, N. Mohan, and T. Undeland, "Control of a doubly-fed induction wind generator under unbalanced grid voltage conditions," in *Proc. Eur. Conf. Power Electron. Appl.*, 2005.

[36] J.-B. Hu, Y.-K. He, and H. Nian, "Enhanced control of DFIG-used back-to-back PWM VSC under unbalanced grid voltage conditions," *J. Zhejiang Univ.-Sci. A*, vol. 8, no. 8, pp. 1330–1339, Jul. 2007.

[37] X.-B. Kong and X.-J. Liu, "Nonlinear model predictive control for DFIG-based wind power generation," *Acta Autom. Sinica*, vol. 39, no. 5, pp. 636–643, Mar. 2014.

[38] J.-I. Jang, Y.-S. Kim, and D.-C. Lee, "Active and reactive power control of DFIG for wind energy conversion under unbalanced grid voltage," in *Proc. 5th Int. Power Electron. Motion Control Conf.*, vol. 3, Aug. 2006, pp. 1487–1491.

ALI M. ELTAMALY received the B.Sc. and M.Sc. degrees in electrical engineering from Al-Minia University, Egypt, in 1992 and 1996, respectively, and the Ph.D. degree in electrical engineering from Texas A&M University, in 2000. He is currently a Full Professor with King Saud University, Saudi Arabia, and Mansoura University, Egypt. He has supervised several of M.Sc. and Ph.D. theses, and worked on number of technical projects. He has published 15 books and book chapters, and he has authored or coauthored more than 200 refereed journal articles and conference papers, as well as a number of patents with the U.S. Patent Office. His current research interests include renewable energy, smart grids, power electronics, motor drives, power quality, artificial intelligence, evolutionary and heuristic optimization techniques, and distributed generation. He received a professor award for scientific excellence from Egyptian Supreme Council of Universities, Egypt, in June 2017, and he has been awarded many prizes from different universities in Egypt and Saudi Arabia. He has Chaired many international conference sessions. He participates as an Editor and Associate Editor for many international journals.

M. S. AL-SAUD received the Ph.D. degree from McMaster University, Canada, in 2007. He is currently an Associate Professor with the Electrical Engineering Department, King Saud University. He is also the Director of the Saudi Electricity Company Chair in Power System Reliability and Security. As part of his work at King Saud University, he has been involved in research and development activities in the areas of sustainable energy technologies, smart grid and renewable energy adoption, reliability and security assessment of power supply systems, design and operation of distribution systems, application of artificial intelligence in power system design, and load management.

AHMED G. ABO-KHALIL received the bachelor's and M.Sc. degrees in engineering from Assiut University, Egypt, and the Ph.D. degree from the School of Electrical and Computer Engineering, Yeungnam University, South Korea, in 2007. In 2008, he joined the Rensselaer Polytechnic Institute, NY, USA, as a Postdoctoral Researcher, and worked on a renewable energy project. From 2009 to 2010, he was a Postdoctoral Research Fellow with the Korean Institute of Energy Research, Daejeon, South Korea, working on photovoltaic power conversion systems. In 2010, he moved to Assiut University as an Assistant Professor. He currently works as an Associate Professor with the Department of Electrical Engineering, Majmaah University, Almajmaah, Saudi Arabia.